



# **Determining the Best Hail Global Solar Radiation Model**

Prepared by:

Abdulmajeed Alsharari

ID # 439026055

Supervised by:

Prof. Ahmad Alkaoud

Physics Department, College of Science  
Imam Muhammad ibn Saud Islamic  
University (IMSIU)

Prof. Zaki Al-Mostafa

The National Astronomy Center  
King Abdulaziz City for Science and Technology  
(KACST)

3<sup>rd</sup> Semester 1446 AH

## **Abstract**

Numerous experimental models have been established to predict solar radiation patterns. Among these, daily sunshine duration is the most widely utilized parameter due to its straightforward and consistently measurable nature. In this study, 52 models that are variants of the Angstrom-Prescott model were evaluated to estimate the monthly mean global solar radiation incident on horizontal surfaces. These models were applied to publicly accessible meteorological datasets for Ha'il, Saudi Arabia. The analysis revealed significant differences in model performance, with certain models proving inadequate for the region. Ultimately, the optimal model for accurate solar radiation estimation in Ha'il was identified.

## **Acknowledgment**

In the beginning, my heartfelt thanks go to my esteemed advisors, Prof. Zaki Al-Mostafa and Prof. Ahmad Alkaoud, for their insightful guidance, continuous encouragement, and unwavering support throughout this research. I want also to express my sincere gratitude to the King Abdulaziz City for Science and Technology (KACST) for their generous support in facilitating this work. I want to extend my deepest appreciation to the Physics Department for providing an excellent research environment and valuable resources. I am also profoundly grateful to my family for their endless patience, love, and motivation, which have been instrumental in my academic journey. Finally, I acknowledge my colleagues and peers for their stimulating discussions, constructive feedback, which greatly enriched this work.

# 1. Introduction and Literature Review

## 1.1 Solar Radiation

### 1.1.1 Global Solar Radiation

Global solar radiation (GSR) is a critical component of the Earth's energy balance and plays a vital role in atmospheric processes, climate dynamics, and renewable energy production. It refers to the total amount of shortwave radiation received from the sun on a horizontal surface at the Earth's surface, including both direct sunlight and diffuse sky radiation. Understanding and accurately measuring GSR is essential for applications in agriculture, meteorology, solar energy system design, and climate modeling.

Global solar radiation is composed of two main components:

1. Direct Solar Radiation (Beam Radiation): This is the portion of sunlight that travels in a straight path from the sun to the Earth's surface without being scattered or absorbed by the atmosphere.
2. Diffuse Solar Radiation: This component results from sunlight that has been scattered by molecules, aerosols, and clouds in the atmosphere and reaches the surface from all directions.

The sum of these two components on a horizontal surface is termed **Global Solar Radiation (GSR)**. Mathematically, it is expressed as:

$$G = D + S$$

where  $G$  is the global radiation,  $D$  is the diffuse radiation, and  $S$  is the direct radiation component projected onto a horizontal surface.

### 1.1.2 Measurements of Global Horizontal Solar Radiation

GSR is typically measured using pyranometers, which are radiometric instruments designed to measure the solar irradiance received from the hemisphere above. These devices often employ a thermopile sensor beneath a glass dome to detect the incoming solar energy across a broad spectrum (approximately 300 to 3000 nm). Calibration and maintenance are essential to ensure accuracy, and measurements are often collected in real-time and averaged over hourly or daily intervals.

Satellite-based measurements and numerical models are also used to estimate GSR over large spatial scales. These methods integrate atmospheric parameters such as cloud cover, aerosol concentration, and water vapor content to produce high-resolution solar radiation maps.

### 1.1.3 Factors Affecting Horizontal Global Solar Radiation

Several factors influence the amount of global solar radiation reaching the Earth's surface:

- **Latitude:** Solar radiation varies with latitude due to the curvature of the Earth and the angle of solar incidence.
- **Season and Time of Day:** The solar zenith angle changes throughout the day and year, affecting the intensity of received radiation.
- **Cloud Cover:** Clouds can significantly reduce direct radiation and increase the diffuse component.
- **Aerosols and Atmospheric Composition:** Dust, pollutants, and water vapor in the atmosphere absorb and scatter incoming solar radiation.
- **Surface Albedo:** The reflectivity of the Earth's surface also plays a role in modulating the effective solar energy absorbed.

### 1.1.4 Applications of Global Solar Radiation Data

1. **Renewable Energy Systems:** GSR data is critical for the optimal design, performance assessment, and economic feasibility of solar photovoltaic (PV) systems and solar thermal installations. Energy yield calculations rely heavily on historical and real-time radiation data.
2. **Climate Studies:** GSR is a key variable in climate models as it influences surface temperature, evapotranspiration, and atmospheric circulation.
3. **Agricultural Planning:** Knowledge of solar radiation patterns helps in predicting crop yield, irrigation needs, and photosynthetic activity.
4. **Building Design:** In passive solar building designs, accurate GSR estimates are used to optimize window placement, thermal insulation, and daylighting strategies.

### 1.1.5 Ha'il Region: Geographical and Solar Radiation Context

Ha'il is located in the north-central part of Saudi Arabia and spans an area of approximately 118,000 km<sup>2</sup>. According to the Saudi Arabian Solar Radiation Atlas, the region is situated at a latitude of 27°28'N and a longitude of 41°38'E (see Figure 1), with an elevation of about 1,010 meters above sea level. The region is characterized by a diverse terrain that includes vast desert plains and mountainous formations such as

the Aja and Salma mountains. Ha'il's topography and clear skies contribute to a high level of solar exposure throughout the year. The climate is classified as semi-arid, with hot summers, mild winters, and low annual rainfall averaging around 100 mm. These climatic conditions, combined with minimal cloud cover, make Ha'il highly suitable for solar energy applications.

In recognition of this solar potential, Ha'il has become a candidate for solar energy development projects, particularly in off-grid and agricultural zones where reliable electricity access is crucial. Data from the Saudi Arabian Solar Radiation Atlas indicates that the region receives average daily global horizontal irradiance (GHI) levels of approximately 5.5 to 6.0 kWh/m<sup>2</sup>/day. The stable solar resource presents opportunities for integrating solar power in local sustainability efforts, including water pumping, greenhouses, and battery storage systems.

Sunshine duration remains the most practical variable for estimating global solar radiation (GSR) in such regions. This is especially relevant for Ha'il, where long sunshine hours are recorded consistently. The original Angstrom equation compares monthly average radiation with extraterrestrial radiation and the fraction of possible sunshine, providing a reliable empirical tool for solar assessment in Ha'il and similar arid regions.



Map data ©2025 Google, Mapa GISrael 200 km

Figure 1: Ha'il Region

## 1.2 Modeling of Global Solar Radiation

### 1.2.1 Angstrom Equation for Global Solar Radiation

One of the most widely used empirical models for estimating solar radiation on the Earth's surface is the Angstrom Equation. Developed by Swedish physicist Anders Knutsson Ångström in the early 20th century, the equation represents a seminal contribution to atmospheric physics and solar radiation modeling. In his influential report to the International Commission for Solar Research in 1924, Ångström proposed a linear relationship between the fraction of possible sunshine duration and the fraction of extraterrestrial solar radiation reaching the Earth's surface (Angstrom, 1924). This formulation laid the foundation for what would become a cornerstone method in solar climatology, particularly useful in locations where direct measurements of solar irradiance are unavailable or limited.

The original form of the Angstrom Equation is expressed as:

$$\frac{H}{H_0} = a + b \left( \frac{S}{S_0} \right)$$

where:

- $H$  is measured or estimated average daily global solar radiation on a horizontal surface (MJ/m<sup>2</sup>/day),
- $H_0$  is the theoretical daily extraterrestrial solar radiation on a horizontal surface,
- $S$  is the actual sunshine duration (hours),
- $S_0$  is the maximum possible sunshine duration or day length (hours),
- $a, b$  are empirical regression coefficients.

This linear equation essentially describes how solar radiation received at the Earth's surface ( $H$ ) is affected by the actual sunshine duration ( $S$ ), relative to the theoretical maximum ( $S_0$ ). The parameters  $a$  and  $b$  are location-dependent and typically derived through regression analysis using long-term solar radiation and sunshine duration datasets. The coefficient  $a$  reflects the portion of solar radiation reaching the surface under completely overcast conditions, while  $b$  reflects the additional radiation gained per unit of sunshine duration.

The Angstrom Equation has proven remarkably robust and adaptable, particularly in climatological and agricultural studies, energy system modeling, and environmental impact assessments. Its simplicity is a key strength: it relies only on readily available meteorological variables, particularly sunshine duration, which has historically been recorded in many weather stations worldwide, even in the absence of direct pyranometer-based solar radiation measurements.

The Angstrom Equation remains a foundational tool in solar radiation estimation. Its development over a century ago marked a pivotal point in the integration of observational meteorology and theoretical solar physics. While modern satellite-based and physically detailed radiative transfer models have become prevalent, the Angstrom model's elegance and empirical power continue to ensure its relevance. Its adaptability, combined with minimal data requirements, makes it indispensable for solar resource assessment, especially in developing regions or areas with limited observational infrastructure.

### 1.2.2 Modifications on the Angstrom Equation

In modern applications, the Angstrom Equation often serves as a baseline model or is integrated into more complex estimation frameworks. It has also inspired several modifications, the most notable being the Angstrom-Prescott model, which adjusts and calibrates the  $a$  and  $b$  coefficients for improved accuracy in specific geographic or climatic contexts.

Such models are widely used for estimating the solar energy potential of a location, aiding in the design and optimization of photovoltaic systems, solar thermal collectors, and in broader renewable energy planning. Additionally, the equation contributes to agronomic models that assess crop water requirements, photosynthetically active radiation, and evapotranspiration rates.

Despite its practical utility, the Angstrom Equation has limitations. The linear assumption between sunshine duration and global solar radiation can oversimplify the actual physical processes involved, particularly under variable atmospheric conditions such as high aerosol loads, frequent cloud cover, or in regions influenced by seasonal monsoons. Furthermore, the empirical coefficients  $a$  and  $b$  are not universal—they require careful calibration for each specific location and can vary seasonally or due to long-term climate trends.

For example, in arid and semi-arid regions such as northern Saudi Arabia, including the Ha'il region, local calibration becomes essential. Atmospheric dust, humidity variations, and cloud formation patterns influence the performance of the Angstrom Equation, necessitating localized regression studies to obtain accurate predictions. Nevertheless, even in such cases, the model continues to offer valuable insights, especially when direct radiation data is scarce.



### 1.2.3 Angstrom-based Models from the Literature

Models used to calculate the daily monthly average GSR on a horizontal surface have different forms of dependence on the  $S/S_0$  ratio. Al-Mostafa et al investigated 52 models for estimating global solar radiation at Hutat Suder. These models are classified as following. The data are shown in Table I.

The relative percentage error of each model was calculated for each month during the year in Hail.

- I. Group 1 (linear models): It has a shape similar to the Angstrom type regression equation; but the experimental coefficients A and B vary, depending on the results obtained for first-order regression analysis.
- II. Group 2 (second order models): Some researchers have used a quadratic polynomial equation for the  $S/S_0$  ratio to calculate the daily monthly mean GSR on a horizontal surface.
- III. Group 3 (third order models): The monthly average daily GSR is parameterised as a function of the  $S/S_0$  ratio's third order dependence.
- IV. Group 4 (Logarithmic models).
- V. Groups 5 and 6 (Exponential models): These groups include simple power equations and exponential power equations.
- VI. Group 7 (Angular models).

## 1.3 Project Objectives

The main objective of this work is to investigate the suitability of Angstrom-based models when they are applied on Ha'il solar radiation data. The best model will be identified based on the error calculations.

## 2. Methodology

### 2.1. Ha'il Solar Data

The solar radiation data of Ha'il region is routinely published by King Abdulaziz City for Science and Technology (KACST) in the Saudi Arabia Solar Radiation Atlas. The first Atlas was published in 1983. In 1998, in collaboration with the National Renewable Energy Laboratory, the 2<sup>nd</sup> Atlas was published. The solar radiation data of Hail region are summarized in Table 1. Figure 2 shows the data plot. As can be seen, there is parabolic shape behavior in most of the data except for April and November, which deviate from the parabolic pattern.

Month	S (hour)	S <sub>0</sub> (hour)	S/S <sub>0</sub>	H (kW)	H <sub>0</sub> (kW)	H/H <sub>0</sub>
1.00	7.1	10.5	0.676	3.464	6.355	0.545
2.00	8.6	11.1	0.775	4.453	7.579	0.588
3.00	8.6	11.9	0.723	5.229	9.083	0.576
4.00	9.2	12.7	0.724	6.194	10.36	0.598
5.00	10.2	13.4	0.761	6.424	11.106	0.578
6.00	11.6	13.7	0.847	6.787	11.361	0.597
7.00	11.9	13.6	0.875	6.596	11.21	0.588
8.00	11.5	13	0.885	6.22	10.629	0.585
9.00	9.6	12.2	0.787	5.633	9.575	0.588
10.00	9.1	11.4	0.798	4.819	8.134	0.592
11.00	8.1	10.7	0.757	3.659	6.725	0.544
12.00	7.7	10.3	0.748	3.358	5.983	0.561



Figure 2: Solar Radiation Data of Ha'il Region

## 2.2 Angstrom-based Solar Radiation Models

Below is the list of models that will be tested and applied on Ha'il radiation data:

Model No.	Model Formula
1	$\frac{H}{H_o} = 0.6307 - 0.7251 \left(\frac{S}{S_o}\right) + 1.2089 \left(\frac{S}{S_o}\right)^2 - 0.4633 \left(\frac{S}{S_o}\right)^3$
2	$\frac{H}{H_o} = 0.1520 - 1.1334 \left(\frac{S}{S_o}\right) - 1.1126 \left(\frac{S}{S_o}\right)^2 + 0.4516 \left(\frac{S}{S_o}\right)^3$
3	$\frac{H}{H_o} = 0.1874 + 0.8591 \left(\frac{S}{S_o}\right) - 0.4764 \left(\frac{S}{S_o}\right)^2$
4	$\frac{H}{H_o} = 0.3078 + 0.4166 \left(\frac{S}{S_o}\right)$
5	$\frac{H}{H_o} = 0.3398 + 0.2868 \left(\frac{S}{S_o}\right) + 0.1187 \left(\frac{S}{S_o}\right)^2$
6	$\frac{H}{H_o} = 0.4832 - 0.6161 \left(\frac{S}{S_o}\right) + 1.8932 \left(\frac{S}{S_o}\right)^2 - 1.0975 \left(\frac{S}{S_o}\right)^3$
7	$\frac{H}{H_o} = 0.324 + 0.405 \left(\frac{S}{S_o}\right)$
8	$\frac{H}{H_o} = 0.348 + 0.320 \left(\frac{S}{S_o}\right) + 0.070 \left(\frac{S}{S_o}\right)^2$
9	$\frac{H}{H_o} = -0.0271 + 0.3096 \exp \left(\frac{S}{S_o}\right)$
10	$\frac{H}{H_o} = 0.2854 + 0.2591 \left(\frac{S}{S_o}\right) + 0.6171 \left(\frac{S}{S_o}\right)^2 - 0.4834 \left(\frac{S}{S_o}\right)^3$
11	$\frac{H}{H_o} = 0.2671 + 0.4754 \left(\frac{S}{S_o}\right)$
12	$\frac{H}{H_o} = 0.23 + 0.38 \left(\frac{S}{S_o}\right)$
13	$\frac{H}{H_o} = 0.318 + 0.449 \left(\frac{S}{S_o}\right)$
14	$\frac{H}{H_o} = 0.698 + 0.2022 \ln \left(\frac{S}{S_o}\right)$
15	$\frac{H}{H_o} = 0.1541 + 1.1714 \left(\frac{S}{S_o}\right) - 0.705 \left(\frac{S}{S_o}\right)^2$
16	$\frac{H}{H_o} = 0.1796 + 0.9813 \left(\frac{S}{S_o}\right) - 0.2958 \left(\frac{S}{S_o}\right)^2 - 0.2657 \left(\frac{S}{S_o}\right)^3$
17	$\frac{H}{H_o} = 0.3396 e^{0.8985 \left(\frac{S}{S_o}\right)}$
18	$\frac{H}{H_o} = 0.7316 \left(\frac{S}{S_o}\right)^{0.4146}$
19	$\frac{H}{H_o} = 0.3092 \cos(\phi) + 0.4931 \left(\frac{S}{S_o}\right)$ where $\phi$ is the latitude of the site in degrees
20	$\frac{H}{H_o} = 0.2408 + 0.3625 \left(\frac{S}{S_o}\right) + 0.4597 \left(\frac{S}{S_o}\right)^2 - 0.3708 \left(\frac{S}{S_o}\right)^3$
21	$\frac{H}{H_o} = 0.309 + 0.368 \left(\frac{S}{S_o}\right)$
22	$\frac{H}{H_o} = 0.367 + 0.367 \left(\frac{S}{S_o}\right)$
23	$\frac{H}{H_o} = 0.233 + 0.591 \left(\frac{S}{S_o}\right)$
24	$\frac{H}{H_o} = -2.4275 + 11.946 \left(\frac{S}{S_o}\right) - 16.745 \left(\frac{S}{S_o}\right)^2 - 7.9575 \left(\frac{S}{S_o}\right)^3$
25	$\frac{H}{H_o} = 0.2424 + 0.5014 \left(\frac{S}{S_o}\right)$
26	$\frac{H}{H_o} = 0.0959 + 0.9958 \left(\frac{S}{S_o}\right) - 0.3922 \left(\frac{S}{S_o}\right)^2$

Model No.	Model Formula
27	$\frac{H}{H_o} = 0.215 + 0.527 \left( \frac{S}{S_o} \right)$
28	$\frac{H}{H_o} = 0.1 + 0.874 \left( \frac{S}{S_o} \right) - 0.255 \left( \frac{S}{S_o} \right)^2$
29	$\frac{H}{H_o} = 0.148 + 0.668 \left( \frac{S}{S_o} \right) - 0.079 \left( \frac{S}{S_o} \right)^2$
30	$\frac{H}{H_o} = 0.2262 + 0.418 \left( \frac{S}{S_o} \right)$
31	$\frac{H}{H_o} = 0.34 + 0.32 \left( \frac{S}{S_o} \right)$
32	$\frac{H}{H_o} = 0.27 + 0.65 \left( \frac{S}{S_o} \right)$
33	$\frac{H}{H_o} = 0.1538 + 0.7874 \left( \frac{S}{S_o} \right)$
34	$\frac{H}{H_o} = 0.1961 + 0.7212 \left( \frac{S}{S_o} \right)$
35	$\frac{H}{H_o} = 0.41 + 0.57 \left( \frac{S}{S_o} \right)$
36	$\frac{H}{H_o} = 0.81 - 3.34 \left( \frac{S}{S_o} \right) + 7.38 \left( \frac{S}{S_o} \right)^2 - 4.51 \left( \frac{S}{S_o} \right)^3$
37	$\frac{H}{H_o} = 0.225 + 0.014 \left( \frac{S}{S_o} \right) + 0.001 \left( \frac{S}{S_o} \right)^2$
38	$\frac{H}{H_o} = -0.14 + 2.52 \left( \frac{S}{S_o} \right) - 3.71 \left( \frac{S}{S_o} \right)^2 + 2.24 \left( \frac{S}{S_o} \right)^3$
39	$\frac{H}{H_o} = 0.313 + 0.474 \left( \frac{S}{S_o} \right)$
40	$\frac{H}{H_o} = 0.307 + 0.488 \left( \frac{S}{S_o} \right)$
41	$\frac{H}{H_o} = 0.309 + 0.599 \left( \frac{S}{S_o} \right)$
42	$\frac{H}{H_o} = 0.335 + 0.367 \left( \frac{S}{S_o} \right)$
43	$\frac{H}{H_o} = 0.388 \cos(\emptyset) + 0.367 \left( \frac{S}{S_o} \right)$
44	$\frac{H}{H_o} = 0.241 + 0.488 \left( \frac{S}{S_o} \right)$
45	$\frac{H}{H_o} = 0.240 + 0.513 \left( \frac{S}{S_o} \right)$
46	$\frac{H}{H_o} = -0.309 + 0.539 \cos(\emptyset) - 0.0693Z + 0.290 \left( \frac{S}{S_o} \right) + \left( 1.527 - 1.027 \cos(\emptyset) + 0.0926Z - 0.359 \left( \frac{S}{S_o} \right) \right)$
47	$\frac{H}{H_o} = 0.195 + 0.676 \left( \frac{S}{S_o} \right) - 0.142 \left( \frac{S}{S_o} \right)^2$
48	$\frac{H}{H_o} = 0.18 + 0.60 \left( \frac{S}{S_o} \right)$
49	$\frac{H}{H_o} = 0.24 + 0.53 \left( \frac{S}{S_o} \right)$
50	$\frac{H}{H_o} = 0.191 + 0.571 \left( \frac{S}{S_o} \right)$
51	$\frac{H}{H_o} = 0.297 + 0.432 \left( \frac{S}{S_o} \right)$
52	$\frac{H}{H_o} = 0.262 + 0.454 \left( \frac{S}{S_o} \right)$

## 2.3 Error Estimation Methods

In the validation of empirical models for estimating global solar radiation, statistical error metrics play a crucial role in evaluating prediction accuracy and consistency. The following five metrics are most widely used in solar energy studies:

### 1. Mean Bias Error (MBE)

MBE measures the average deviation between predicted and observed values. It reflects the tendency of a model to overestimate or underestimate actual measurements, according to the following formula:

$$MBE = \frac{1}{N} \sum_{i=1}^N (H_{iAtlas} - H_{iModel})$$

### 2. Root Mean Square Error (RMSE)

RMSE quantifies the square root of the average squared differences between predicted and observed values. It emphasizes larger deviations and is sensitive to outliers, according to the following formula:

$$RMSE = \sqrt{\frac{1}{N} \sum_{i=1}^N (H_{iAtlas} - H_{iModel})^2}$$

### 3. Mean Percentage Error (MPE)

MPE computes the average percentage error, offering a relative measure of error. However, its reliability may diminish when observed values are close to zero, according to the following formula:

$$MPE = \frac{1}{N} \sum_{i=1}^N \left( \frac{H_{iAtlas} - H_{iModel}}{H_{iAtlas}} \times 100 \right)$$

### 4. Mean Absolute Bias Error (MABE)

MABE evaluates the average of absolute differences between predicted and observed values, providing a straightforward metric for model accuracy according to the formula:

$$MABE = \frac{1}{N} \sum_{i=1}^N |H_{iAtlas} - H_{iModel}|$$

These statistical tools are essential for comparing and optimizing solar radiation models, especially under varying climatic and geographical conditions.

### 3. Data Analysis

The error metrics above were applied on all models. The results are shown in Table 2 below.

MABE	MPE	RMSsq	RMSE	MBE	MODEL NAME	MODEL #
0.13	0.69	0.18	0.03	0.03	BAKIRCI 3	1
0.16	-2.02	0.19	0.03	-0.13	TAHRAN&SARI2	2
0.12	-0.71	0.15	0.02	-0.05	TAHRAN&SARI3	3
0.51	9.65	0.57	0.32	0.51	ARAS etal1	4
0.54	10.27	0.62	0.38	0.54	ARAS etal2	5
0.48	9.33	0.51	0.26	0.48	ARAS etal3	6
0.57	10.89	0.62	0.39	0.57	AHMAD&ULFAT1	7
0.58	10.99	0.64	0.41	0.58	AHMAD&ULFAT2	8
0.68	12.66	0.81	0.65	0.68	ALMOROX&HONTORIA exp	9
0.56	10.57	0.63	0.40	0.56	ULGEN&HEPBASLI1	10
0.49	9.42	0.52	0.27	0.49	ULGEN&HEPBASLI3	11
0.46	-8.76	0.50	0.25	-0.46	AKPABIO&ETUK1	12
0.83	15.80	0.89	0.78	0.83	TOGRUL&TOGRUL1	13
0.62	12.09	0.65	0.42	0.62	TOGRUL&TOGRUL1LN	14
0.50	10.13	0.51	0.26	0.50	TOGRUL&TOGRUL2	15
0.49	9.99	0.50	0.25	0.49	TOGRUL&TOGRUL3	16
1.00	18.85	1.09	1.19	1.00	TOGRUL&TOGRULexp	17
0.74	14.26	0.78	0.61	0.74	TOGRUL&TOGRUL ^	18
3.65	-70.36	3.73	13.94	-3.65	ULGEN&HEPBASIL1	19
0.44	8.43	0.49	0.24	0.44	ULGEN&HEPBASIL3	20
0.20	3.28	0.26	0.07	0.17	CHEGAAR&CHIBANI11	21
0.69	13.18	0.73	0.53	0.69	CHEGAAR&CHIBANI12	22
1.07	20.32	1.16	1.34	1.07	CHEGAAR&CHIBANI13	23
0.81	-15.64	0.86	0.74	-0.81	ERTEKIN&YALDIZ3	24
0.52	9.82	0.60	0.36	0.52	ULGEN&OZBALTA1	25
0.50	9.61	0.55	0.30	0.50	ULGEN&OZBALTA2	26
0.46	8.54	0.55	0.30	0.46	SAID1	27
0.45	8.45	0.52	0.27	0.45	SAID2	28
0.42	7.62	0.51	0.26	0.41	AKSOY2	29
0.25	-4.28	0.31	0.09	-0.22	TIRIS etal1	30
0.25	-4.28	0.31	0.09	-0.22	TIRIS etal1	30
0.15	2.15	0.20	0.04	0.11	VEERAN&KUMAR11	31
1.83	34.71	1.92	3.68	1.83	VEERAN&KUMAR12	32
1.76	33.20	1.87	3.51	1.76	GOPINATHAN&SOLER11	33
1.67	31.56	1.77	3.14	1.67	GOPINATHAN&SOLER12	34
0.22	1.38	0.31	0.10	0.09	LEWIS 1	35
0.38	-6.17	0.47	0.22	-0.37	LEWIS 3	36
3.10	-59.06	3.20	10.21	-3.10	TASDEMIROGLU&SEVER2	37
3.11	59.06	3.26	10.60	3.11	SAMUEL3	38
0.40	7.65	0.45	0.20	0.40	JAIN11	39
1.01	19.18	1.07	1.14	1.01	JAIN12	40
1.82	34.55	1.90	3.61	1.82	JAIN13	41
0.40	7.65	0.45	0.20	0.40	RAJA&TWIDELL1	42
0.48	9.25	0.53	0.28	0.48	RAJA&TWIDELLcos1	43
0.41	7.76	0.50	0.25	0.41	LUHANGA&ANDRINGA1	44
0.58	10.97	0.66	0.44	0.58	JAIN&JAIN1	45
0.74	14.20	0.80	0.63	0.74	GOPINATHAN cos2	46
0.53	10.12	0.60	0.36	0.53	OGELMAN2	47
0.66	12.36	0.76	0.58	0.66	BENSONetal11	48
0.70	13.27	0.78	0.61	0.70	BENSONetal12	49
0.55	10.34	0.65	0.42	0.55	KHOLAGIetal11	50
0.52	9.87	0.58	0.34	0.52	KHOLAGIetal12	51
0.37	6.79	0.44	0.20	0.36	KHOLAGIetal13	52

As can be seen in the table, there is a wide variation in error with different models. The minimum error occurred at models No. 1, 2, 3 and 31. Figure 3 and Figure 4 show the hisotgrams of error metrics for all models.

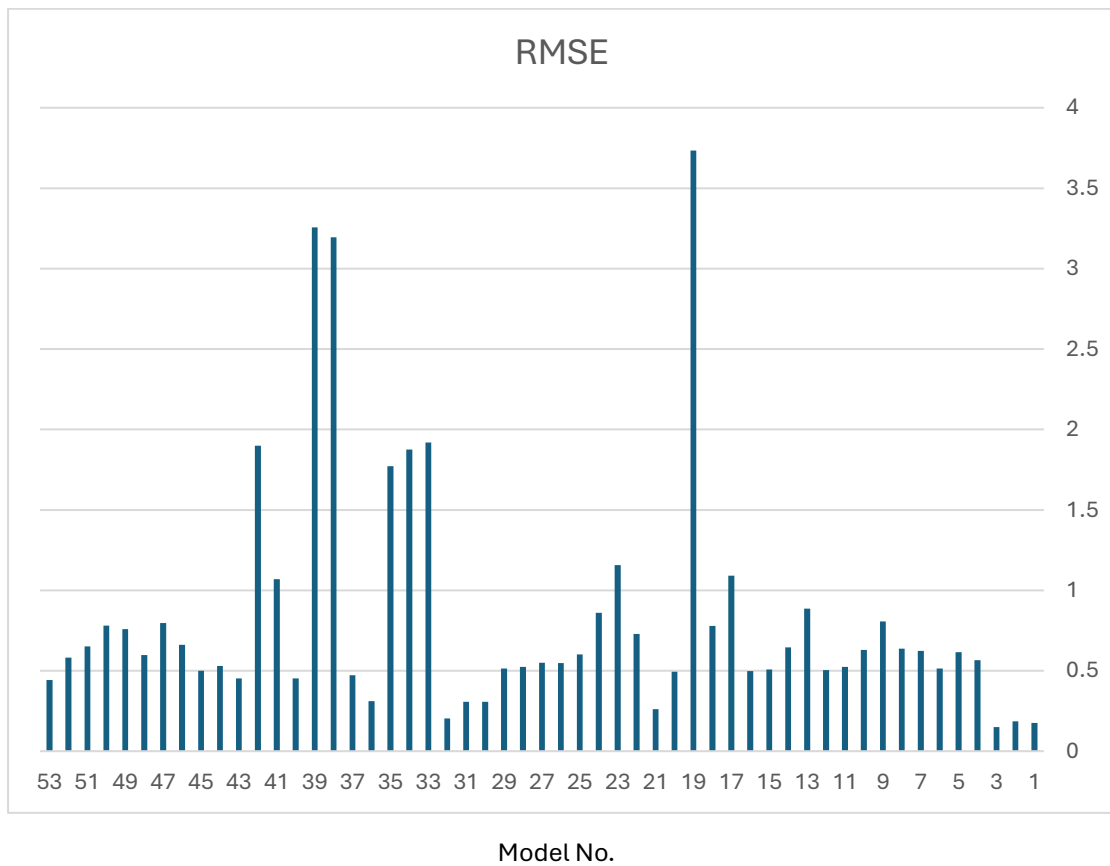
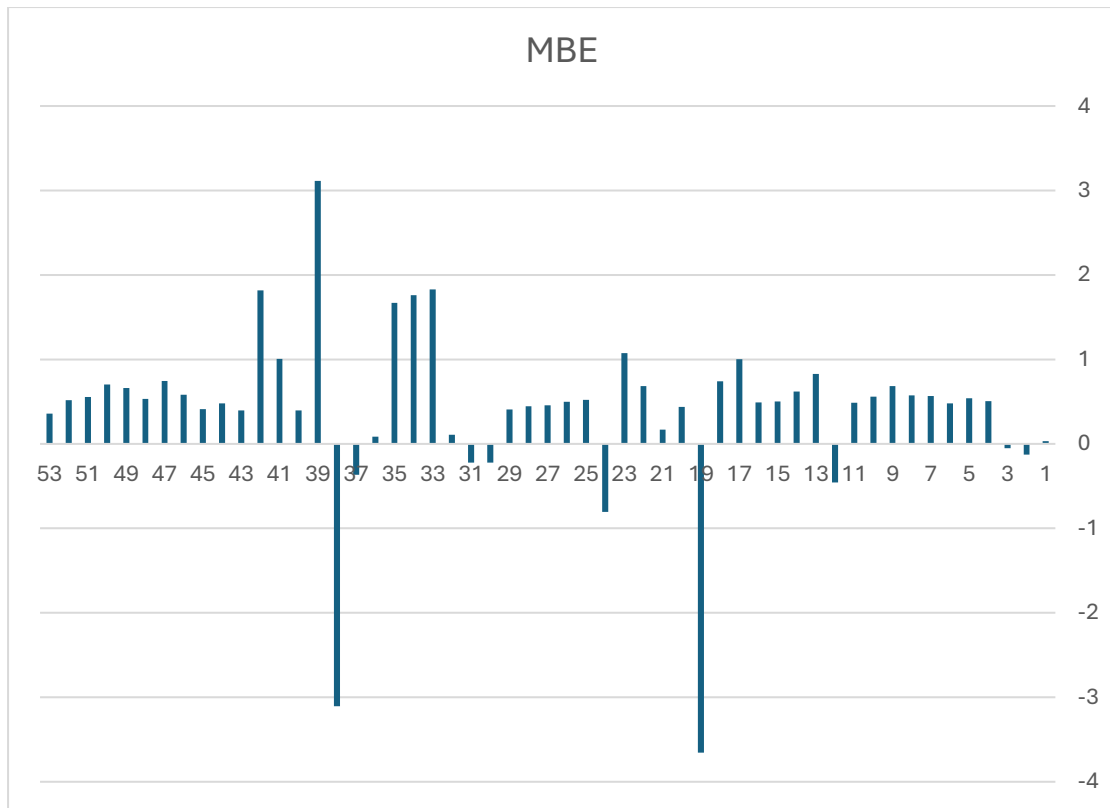


Figure 3: MBE and RMSE errors of models on Ha'il solar radiation

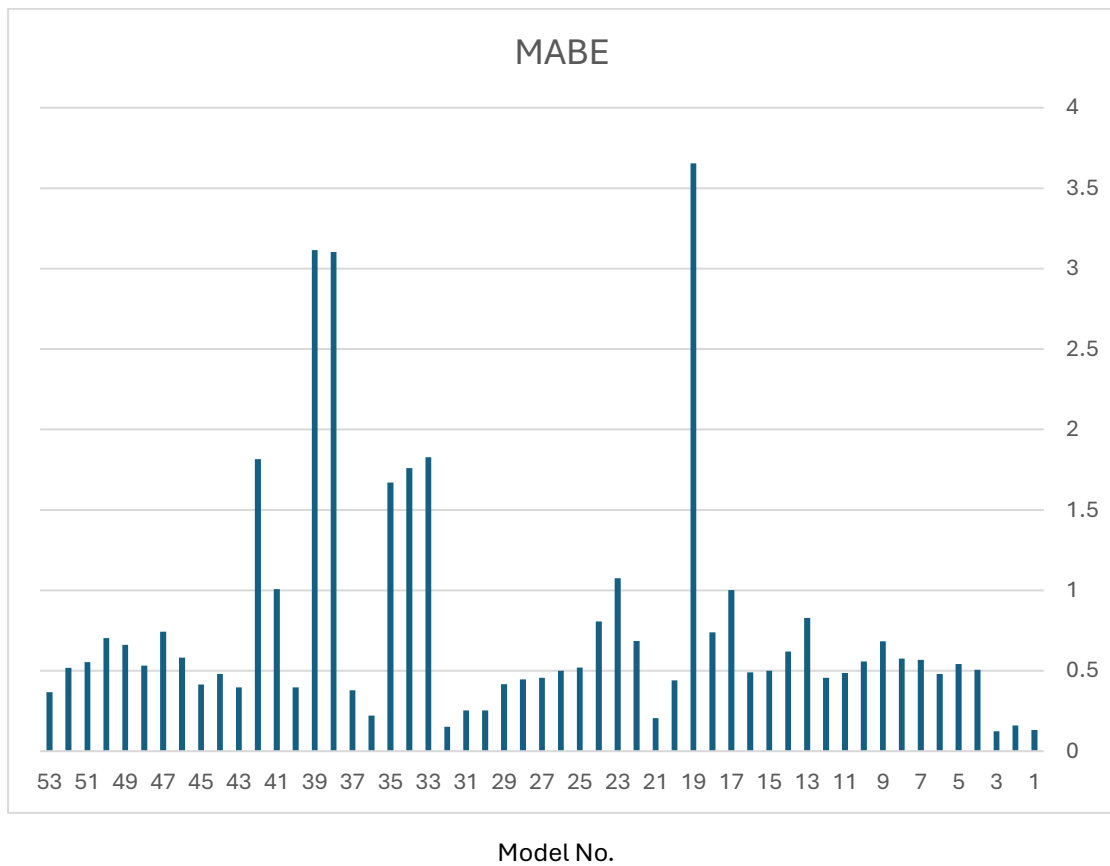
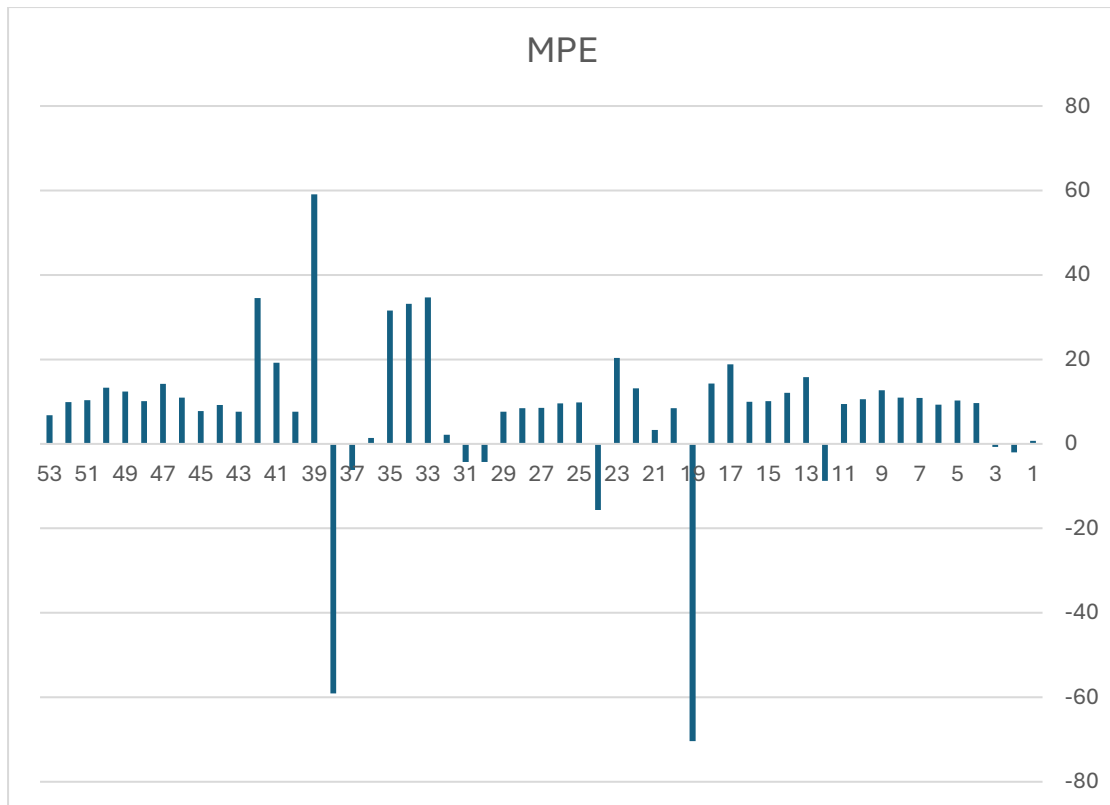


Figure 4: MPE and MABE errors of models on Ha'il solar radiation



A closer investigation of the successful models give us the following:

- I. Models 1 and 2 are 3<sup>rd</sup> order polynomials
- II. Model 3 is a 2<sup>nd</sup> order polynomial
- III. Model 31 is a first order polynomial

When we have a closer look at the Ha'il solar radiation data, except for Months April and Nov, the overall pattern looks more quadratic. Therefore, Model is the preferred model, which has the following form:

$$\frac{H}{H_o} = 0.1874 + 0.8591 \left( \frac{S}{S_o} \right) - 0.4764 \left( \frac{S}{S_o} \right)^2$$

## 4. Conclusion

In the comparative analysis of 52 different global solar radiation models using four statistical performance indicators—MBE, RMSE, MPE, and MABE—Model 3 emerged as the most reliable and accurate for the Hail region. This model showed:

- The lowest RMSE and RMS, indicating a minimal average deviation from the measured values.
- Near-zero MBE, suggesting no systematic overestimation or underestimation bias.
- The lowest MPE and MABE, which reflect both the relative and absolute prediction errors.
- It also has the quadratic form that mimics the behavior of most Ha'il solar cell data.

In the future, work will be extended to model the Ha'il data with a new model in order to reach further error reduction.

## 5. References

1. BSRN. (2023). Baseline Surface Radiation Network. Retrieved from <https://bsrn.awi.de/>
2. Gueymard, C. A. (2004). The sun's total and spectral irradiance for solar energy applications and solar radiation models. *Solar Energy*, 76(4), 423–453. <https://doi.org/10.1016/j.solener.2003.08.039>
3. Duffie, J. A., & Beckman, W. A. (2013). *Solar Engineering of Thermal Processes* (4th ed.). Wiley.
4. WMO. (2008). *Guide to Meteorological Instruments and Methods of Observation* (WMO-No. 8). World Meteorological Organization.
5. Angstrom, A. (1924). Solar and terrestrial radiation: Report to the International Commission for Solar Research on actinometric investigations of solar and atmospheric radiation. *Quarterly Journal of the Royal Meteorological Society*, 50(210), 121–126. <https://doi.org/10.1002/qj.49705021008>
6. Ineichen, P., & Perez, R. (2002). A new airmass independent formulation for the Linke turbidity coefficient. *Solar Energy*, 73(3), 151–157. [https://doi.org/10.1016/S0038-092X\(02\)00045-2](https://doi.org/10.1016/S0038-092X(02)00045-2)
7. H. Al-Sholigom and Z. Al-Mostafa (2024). Identifying the Best Global Solar Radiation Model for Hutat Suder, Saudi Arabia. *International Journal of Physical and Mathematical Sciences*, 18(7): 64-73.
8. General Authority for Statistics, KSA. (2021).
9. Kingdom of Saudi Arabia Solar Radiation Atlas. (1998). Energy Research Institute, Riyadh, SA and National Renewable Energy Laboratory, Colorado, USA. Retrieved from <https://digital.library.unt.edu/ark:/67531/metadc690351/>

10. Saudi Arabian National Center for Science and Technology (SANCST). Saudi Arabian Solar Radiation Atlas; 1983.
11. Mekhlouf, S., Rezzoug, A., & Gama, A. (2020). Empirical Models for Estimating Global Solar Radiation: Review and Comparison. *Renewable and Sustainable Energy Reviews*, 133, 110301.
12. Shen, W., Chen, X., Qiu, J., Hayward, J. A., Sayeef, S., Osman, P., ... & Dong, Z. Y. (2020). A comprehensive review of variable renewable energy levelized cost of electricity. *Renewable and Sustainable Energy Reviews*, 133, 110301.
13. El-Sebaili, A.A., Trabea, A.A. (2005). Estimation of global solar radiation on horizontal surfaces over Egypt. *Energy Conversion and Management*, 46(4), 597–605. <https://doi.org/10.1016/j.enconman.2004.04.008>